Model for the analysis of enzymatic proton-transfer reactions with an application to soybean lipoxygenase-1 and six mutants

Siebrand, Willem; Smedarchina, Zorka

Publisher's version / Version de l'éditeur:
https://doi.org/10.1002/poc.1687
Journal of Physical Organic Chemistry, 23, 7, pp. 620-631, 2010-04-26

Special Issue Article

Journal of Physical Organic Chemistry

Received: 4 August 2009, Revised: 16 September 2009, Accepted: 6 January 2010, Published online in Wiley InterScience: 26 March 2010

(www.interscience.wiley.com) DOI 10.1002/poc.1687

Model for the analysis of enzymatic proton-transfer reactions with an application to soybean lipoxygenase-1 and six mutants

Willem Siebrand[a]* and Zorka Smedarchina[a]

A general analytical model is introduced for the analysis of temperature-dependent rate constants in enzymatic hydrogen and deuterium transfer reactions. It exploits the relationship between kinetic isotope effects (KIEs) and their temperature dependence in tunneling reaction to derive criteria that indicate whether a data set can be assigned to one rate-determining tunneling step in the enzymatic reaction sequence. If so, the model evaluates the relative contributions of the tunneling mode and supporting skeletal modes to transfer and provides information on these modes. Recently reported kinetic data on proton transfer in linoleic acid catalyzed by soybean lipoxygenase-1 (SLO1) and six mutants are analyzed by the model, which includes two oscillators, one representing proton motion relative to the skeletal framework and the other the supporting framework motions. It is concluded that most but not all components of this data set can be assigned to a single tunneling step, possible exceptions being associated with the highest observed rates, in agreement with evolutionary expectations. This still allows a complete analysis, namely in terms of the deuteron rate constants. The analysis evaluates how the contributions to proton transfer of the two modes and the electronic term depend on transfer distances in the enzyme and its mutants. It also provides rationalizations for several apparent anomalies, such as the vanishing of the activation energy for some mutants and the observed invariance of the KIE among mutants with very different activity.

Keywords: enzymatic proton-transfer; kinetic isotope effects; soybean lipoxygenase-1; tunneling

INTRODUCTION

In chemical reactions, protons behave as light particles in the sense that their wave character influences their transfer properties. In practice, this means that when encountering a potential-energy barrier, a proton, unlike a heavier particle, is not restricted to going over the top but may tunnel through. Whether tunneling offers a kinetic advantage depends on the thermal energy. If it is of the order of the barrier height, little is gained by tunneling, but if it is much smaller, tunneling is the only practical transfer mechanism. Barriers will generally be high if the proton is part of a strong bond that needs to be broken. In this contribution we consider cleavage of a CH bond, specifically cleavage catalyzed by enzymes under biological conditions. In view of the strength of the bond and its low polarity, this cleavage is likely to be obstructed by a high barrier. The reaction therefore requires a strong catalyst that can weaken the bond and thereby lower the barrier for cleavage and stabilize the final state to a level where the thermal energy is large enough for the proton to escape from the bond. We may reasonably assume that the evolution of suitable enzymes has been a gradual process aimed at meeting minimum requirements, i.e., at lowering the barrier just enough to allow the proton to tunnel through it at a biologically acceptable rate or, more specifically, at a rate as close as possible to that of the next-slowest step in the enzymatic reaction sequence.

A rough measure of the extent to which tunneling accelerates the reaction is obtained if we replace the moving proton by a deuteron, which has twice the mass and thus will tunnel much more slowly. If this greatly reduces the rate, it appears that the tunneling step is rate limiting. However, as a natural consequence of evolution, rate-limiting steps tend to get faster and to evolve toward a rate comparable to that of other steps. Hence the observation of even a large kinetic isotope effect (KIE) in an enzymatic reaction does not prove that one measures a property of a single reaction step.

The observation of a KIE offers the investigator two different rate constants for essentially the same reaction. The question we wish to address in this contribution is how one can use the extra rate constant to obtain additional information on the reaction. The standard analysis is based on Arrhenius plots of the rate constants against the inverse temperature for a narrow range of temperatures in order to derive effective activation energies, but it typically goes no further than the obvious conclusion that the reaction involves tunneling. Computational efforts based on elaborate, and hence not very transparent, calculations of the KIE, usually at a single temperature, tend to be more suited to test theoretical methods than to analyze experimental data, as key

* *Correspondence to: W. Siebrand, Steacie Institute for Molecular Sciences, National Research Council of Canada, Ottawa, Ontario K1A 0R6, Canada. E-mail: willem.siebrand@nrc-cnrc.gc.ca*

a *W. Siebrand, Z. Smedarchina*
Steacie Institute for Molecular Sciences, National Research Council of Canada, Ottawa, Ontario K1A 0R6, Canada

Journal of Physical Organic Chemistry

questions, such as whether the observations are indeed those of a single step in the reaction sequence, are rarely considered. Given the complexity of enzymatic reactions and our present level of understanding, it seems more profitable to start from the data and look for models that can relate them in a simple and direct manner to physical parameters.

Experimentally, these data are obtained by measuring the rate at which a specific intermediate appears or disappears during the reaction of a substrate with a cleavable CH or CD bond. The rate of the tunneling step will tend to increase with temperature for two different reasons. If the reaction is up-hill, the endothermicity $\Delta E^0 = E_f^0 - E_i^0$, i.e., the difference between the minima of the two wells, enters the rate expression as a Boltzmann factor; this factor is the same for both hydrogen isotopes. In addition, whether the reaction is endothermic or exothermic, higher levels of the CH- and CD-stretching vibrations that govern the proton motion will be populated. Their effect should be isotope-dependent; however, the high frequencies of these vibrations imply that their effect on the rate will become significant only at high temperatures and that at room temperature the vibrational proton and even deuteron motions may be taken to be essentially independent of temperature, especially since measurements of the temperature dependence tend to be limited to small temperature intervals and are thus unsuitable for measuring small effects.

The temperature dependence may still be affected, however, by thermal excitation of lower-frequency vibrations coupled to the proton motion. From studies on small molecules it is known that in the generic reaction

$$\text{X-H}\cdots\text{Y} \rightarrow [\text{X}\cdots\text{H}\cdots\text{Y}] \rightarrow \text{X}\cdots\text{H-Y}$$

the vibrations of the (skeletal) atoms across the hydrogen bridge affect proton transfer in two distinct ways, depending on their symmetry. Of course, the actual transfer potential is not symmetric, but in the model it is effectively symmetrized. In this context, symmetric modes are those that cause displacement along the transfer coordinate and thus modulate the tunneling distance. Antisymmetric modes are those of the same symmetry as the transfer mode; they cannot cause displacement along the transfer coordinate but can add to the barrier. The symmetric X···Y-stretching vibration affects proton transfer by reducing the effective under-barrier part of the proton path. If the frequency of this vibration is of the order of the thermal energy or smaller, this contribution will increase with temperature and thus give rise to a temperature-dependent rate constant. The antisymmetric X···Y-stretching vibration does not affect the reaction path, but contributes a Franck–Condon factor to the rate constant, which for low-frequency vibrations is temperature-dependent; it is similar to the Marcus-type exponent describing polar-solvent reorganization. For enzymatic tunneling reactions we can therefore distinguish two contributions to the reaction path: a vibrational proton contribution that is isotope-dependent but (essentially) temperature-independent, and a contribution of (promoting) skeletal vibrations that is temperature-dependent but (essentially) isotope-independent. This temperature dependence is usually expressed as an (effective) activation energy.

This concept allows us to represent the kinetic properties of these reactions by a very simple model and to use this model to test whether the data for a given reaction are consistent with the assumption that they represent a rate-determining tunneling step. Such a test is necessary because, as pointed out above, evolutionary pressure will tend to accelerate the slowest step in a reaction sequence and thus to weaken its rate-determining status. Surprisingly, no such test has as yet been reported. This may be due in part to the scarcity of accurate data. However, recently, Klinman and coworkers[1,2] have taken a great step forward by carrying out kinetic measurements on a series of mutants of the enzyme soybean lipoxygenase-1 (SLO1), which catalyzes proton transfer in linoleic acid. The resulting set of kinetic data on seven closely related enzymes offers the best information available to date to carry out this test and, in general, to explore the mechanism of enzymatic proton transfer. The authors[1,2] have analyzed their data, at least in part, in terms of a two-oscillator model similar to the one mentioned above. However, they did not develop the model to the point where it can test whether their data are indeed representative of a single tunneling step in the reaction sequence. Furthermore, they limited their calculations to skeletal modes with frequencies smaller than the thermal energy.

In this contribution we analyze the data by a different version of the model, which turns out to yield quite different results. The basic two-oscillator model, one oscillator representing the motion of the proton and the other representing the skeletal vibrations that promote transfer, as introduced in our early tunneling studies,[3] is similar to that used by many subsequent investigators.[1,2,4–6] It has been widely used to calculate proton and deuteron tunneling rate constants as a function of temperature, which necessarily involves the introduction of empirical parameters. Here we use a different approach in which the model is stripped down to its essentials, a procedure justified in the Appendix, and used as an analytical tool. This results in a set of analytical formulas which relate relative rate constants and their temperature dependence, not only those for proton *versus* deuteron transfer but also for rate constants between mutants. These formulas, which are easy to apply, probe whether the data set can represent a single tunneling step in a reaction sequence. If so, they can evaluate how the transfer distance and the contribution of the skeletal mode to the tunneling vary with temperature or mutation. As a first application, we analyze the data of Klinman and coworkers[1,2] on SLO1, and obtain new results that demonstrate both the usefulness of the method and the value of the data set as a window on enzymatic tunneling reactions.

SUMMARY OF DATA

Lipoxygenase-1, depicted in Scheme 1, contains a six-coordinated iron ion that alternates between Fe(III) and Fe(II) during the catalytic cycle in which an electron is abstracted from a CH bond of the C-11 methylene group of linoleic acid. This weakens the bond sufficiently to allow transfer of the proton to an OH group coordinated to the iron ion. The fact that the

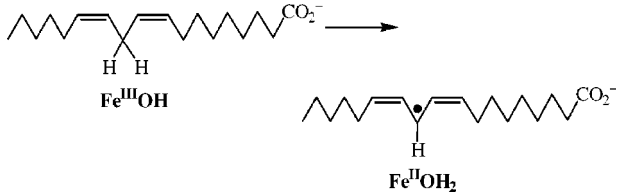

Scheme 1.

electron and the proton involved in the CH-bond cleavage move to different atoms makes the reaction a nonadiabatic (NA) process. Experimentally, the progress of the reaction is followed by product formation, the product being a peroxide formed after proton transfer as an intermediate in the enzymatic reaction. The reported results include the rate constants k_{cat} and the Michaelis constants K_M for hydrogen and deuterium transfer at up to 10 temperatures in the range 278–323 K for the wild-type (WT) enzyme and six mutants. These constants are derived by standard Michaelis–Menten kinetics from the initial rate of product formation under excess substrate conditions:

$$k_{t\to 0} = k_{cat}[SH]/([SH] + K_M) \quad (1)$$

where [SH] is the substrate (hydrogen donor) concentration, $K_M = (k_{-1} + k_{cat})/k_1$, and k_1 and k_{-1} are the association and dissociation rate constants, respectively, of the reactive complex formed by enzyme and substrate. This equation may retain its general form for more complex reaction schemes, including reactions in which the transfer step is reversible. On the basis of the fit to the Michaelis–Menten kinetics, the authors[1,2] assumed that k_{cat} represents the first-order rate constant of a single step in the enzymatic reaction chain, namely the step depicted in Scheme 1. For a detailed description of the reaction and the location of the mutant aminoacid residues, we refer to the original papers [1, 2].

As usual, the observed rate constants $k_{cat}(T)$, supplied as Supporting Information in References [1, 2], are reported in Arrhenius form in the texts:

$$\ln k(T) \simeq \ln \mathcal{A} - E_a/k_B T \quad (2)$$

This is convenient for small temperature intervals, but it should be realized that the Arrhenius equation is fundamentally invalid for tunneling reactions, since their effective activation energy varies from zero for low to the barrier height for high temperatures. As a consequence, the physical meaning of the parameters $\mathcal{A}$ and E_a at temperatures of biological interest is not immediately clear and the same applies to the ratios $\mathcal{A}^D/\mathcal{A}^H$ and E_a^D/E_a^H. In what follows it will be shown that a proper physical interpretation of the latter ratio can be derived for the two-oscillator model. For this purpose, we render E_a dimensionless by expressing it in the thermal energy k_BT, i.e., we modify the Arrhenius plots by replacing T^{-1} by $\ln T^{-1}$ in the abscissa so as to yield, through linear regression, a dimensionless slope $-E_a/k_BT$ instead of $-E_a/k_B$; the corresponding plots are depicted in Figs 1–6 for WT SLO1 and six mutants, and the resulting parameters are listed in Table 1.

Because of the large KIE, a plot of $\ln k$ against $\ln T^{-1}$, as shown in Fig. 1 for the WT enzyme and in Fig. 6 for the two mutants of low activity, tends to be too flat to give a good picture of the accuracy of E_a. Therefore, we show in Figs 2–5 separate plots of proton and for deuteron transfer rate constants for pairs of I553 mutants, arranged so as to yield a clear display. The errors in the $k(T)$ values reported in References [1, 2] correspond to one standard deviation and are typically smaller than the vertical separation of the points from the Arrhenius curve. The errors listed in columns 2, 3, 5, and 6 of Table 1 are newly calculated from linear regression. The errors listed in columns 4 and 7 correspond to the sum of the errors of columns 2 and 3, and of columns 5 and 6, respectively. This summing may underestimate the accuracy, since the KIE is a relative rate constant, which may well lead to compensation of errors of individual rates, as suggested, e.g., by comparison of the KIE of the WT enzyme, the

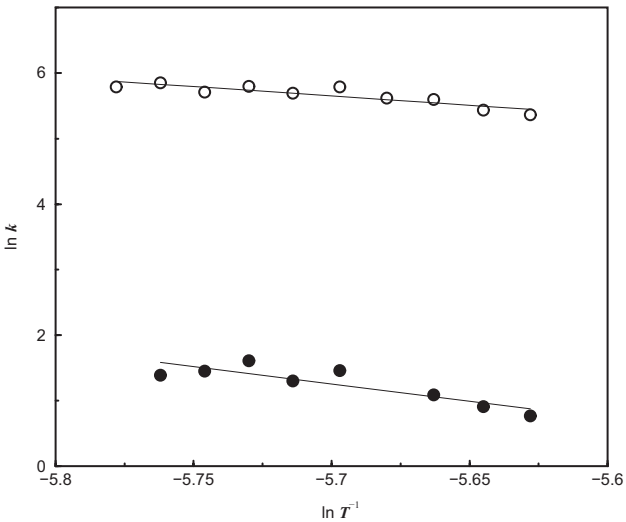

Figure 1. Plot of $\ln k^H$ and $\ln k^D$ *versus* $\ln T^{-1}$ for WT SLO1, based on data taken from Reference [1] (Supporting Information; this holds for all captions). Here and hereafter open symbols refer to H, closed symbols to D

I553A, and the I553L mutant, which have virtually identical rate constants. As may be expected on the basis of the scatter shown by Figs 1–6, the errors near the midpoint of the plots, yielding $\ln k(298)$, are generally smaller than the errors in the slopes, yielding E_a. Since they do not include the errors encountered in the measurements of the individual rate constants, they are probably underestimated.

The KIEs $\eta = k^H/k^D$ are of the order of 100, which proves unequivocally that the reaction proceeds by quantum-mechanical tunneling; however, within the narrow temperature interval probed, the modified Arrhenius plots do not show recognizable deviations from linearity. A remarkable feature of the KIE values is that they vary by less than a factor of 3, while the corresponding proton or deuteron transfer rate constants each cover a range of three orders of magnitude. Within the series

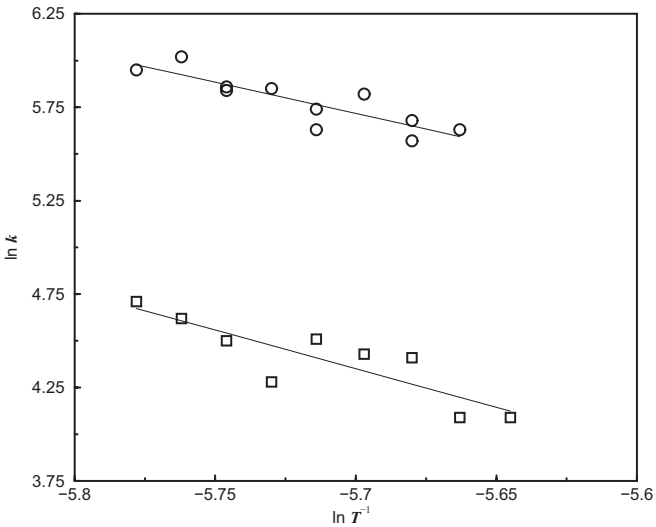

Figure 2. Plot of $\ln k^H$ *versus* $\ln T^{-1}$ for mutants I553A (top) and I553V (bottom), based on data from References [1, 2], respectively

of I553 mutants, where the mutation occurs at a site remote from the reaction center, the rate constants are close to those of the WT enzyme, only those of the I553-V and -G mutants showing a significant reduction. As illustrated in Reference [2], the size of the side chain in the series decreases in the order WT ∼ I553L > I553V > I553A > I553G and hence is not clearly correlated to the rates. With the exception of I553G all mutants exhibit the same KIE as the WT enzyme within the error of the measurements, irrespective of the rate constants, which for the mutants with mutations close to the reaction center, *viz*. L546A and L754A, are, respectively, two and three orders of magnitude smaller than for the others.

In columns 4 and 5 of Table 1, we list the observed activation energies E_a in units $k_BT = 0.59$ kcal/mol for $T = 298$ K. Their small values indicate that the transfer is exothermic. Actually, two of the H-transfer rate constants, namely those of the mutants I553L and I553G, displayed in Fig. 3, are independent of temperature within the error of the measurements,[2] which seems to be incompatible with tunneling at room temperature. While activation energies that are too high may be an indication of endothermicity, there seems to be no easy explanation of an activation energy that is too low. Since the CH- and OH-stretching modes that govern the tunneling have high frequencies, which prevent substantial thermal excitation at room temperature, the temperature dependence will be basically due to contributions of lower-frequency skeletal modes to the reaction. Thus the observation $E_a^H \sim 0$ would appear to imply the absence of such contributions. However, at room temperature many skeletal modes will be thermally excited and their effect on the transfer is clearly shown by the values of E_a^D displayed in Fig. 5; they are about 7 k_BT for these two mutants, similar to those of the other I553 mutants, for which E_a^H is in the range 3–4 k_BT, as shown in Figs 4 and 5. Again, there is no clear correlation with the size of the side chain in the I553 series. For the close mutants L546A and L754A, the activation energies are larger than those for the WT enzyme and the I553 mutants, especially for proton transfer.

Evidently, the available data pose questions that require a more quantitative approach. In Reference [2], an interpretation of the observed properties of the I553 series of mutants is offered based on a model similar to that described in the next section, but not developed so as to allow comparison with all available kinetic observables. Also, it is restricted to the high-temperature limit, where the thermal energy is much larger than the skeletal-mode frequencies. The variation observed in the temperature dependence of the KIE is ascribed to differences in transfer distance, which are claimed to vary from $r_0 = 1.02$ to 3.14 Å. However, this interpretation cannot be correct since the absolute rate constants $k^H(298)$ in the I553 series vary by less than a factor of 6, while the claimed range of transfer distances implies a variation by many orders of magnitude. A significant change of transfer distances is also contradicted by the fact that the mutations occur at a site that is not close to the reaction center. Rather than making any *a priori* assumptions about the causes of the observed differences among the mutants, we choose an approach capable

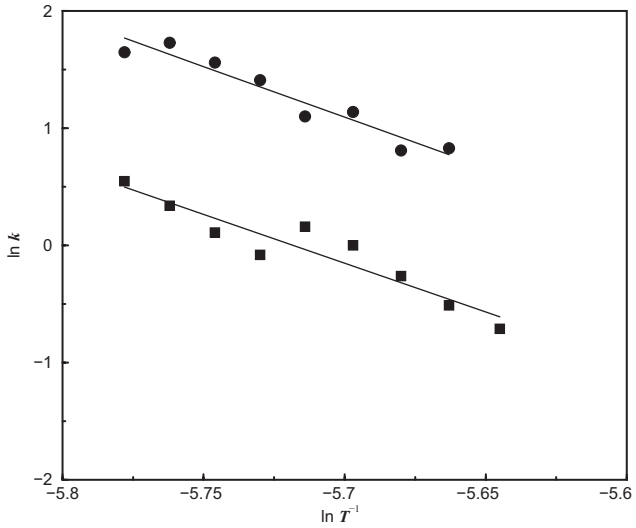

Figure 4. Plot of $\ln k^D$ *versus* $\ln T^{-1}$ for mutants I553A (top) and I553V (bottom), based on data from References [1, 2], respectively

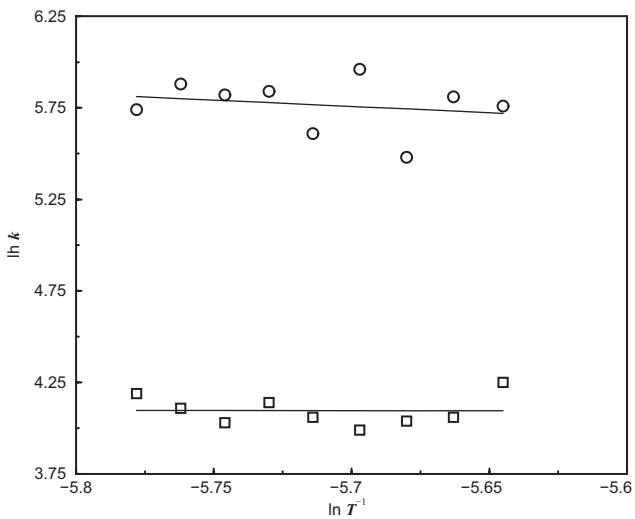

Figure 3. Plot of $\ln k^H$ *versus* $\ln T^{-1}$ for mutants I553L (top) and I553G (bottom), based on data from Reference [2]

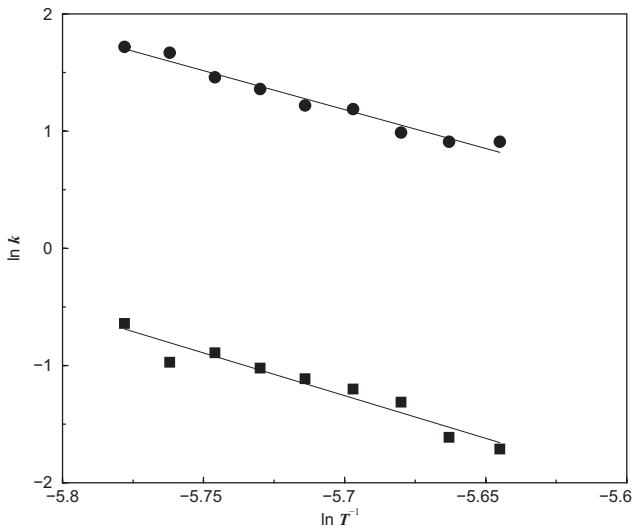

Figure 5. Plot of $\ln k^D$ *versus* $\ln T^{-1}$ for mutants I553L (top) and I553G (bottom), based on data from Reference [2]

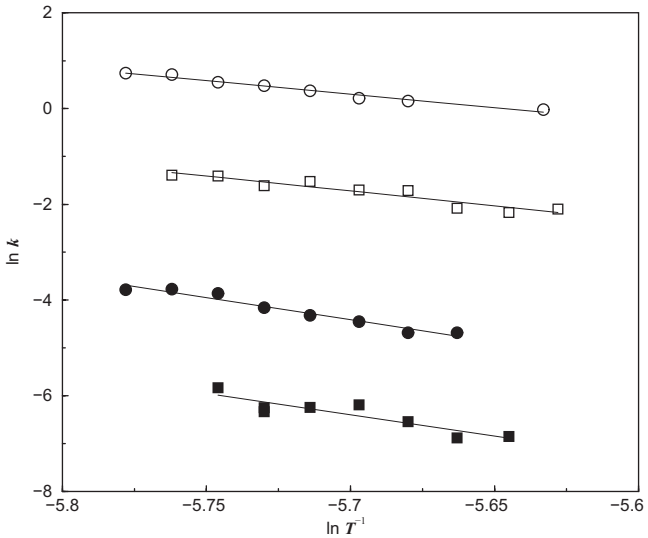

Figure 6. Plot of $\ln k^{H}$ and $\ln k^{D}$ *versus* $\ln T^{-1}$ for mutants L546A (circles) and L754A (squares), based on data from Reference [1]

of providing this information directly in analytic form following substitution of the data.

MODEL

Before transfer the system is assumed to be in the initial state $|i>$ and after transfer in the final state $|f>$, both states being amenable to quantum-chemical evaluation. The coupling driving the transfer, to be specified later, is represented by an operator V; it is obviously weak, since these transfers are much slower than typical molecular vibrations. According to Fermi's Golden Rule, which is always valid if the coupling is time-independent, the transfer rate constant will then be proportional to the square of the matrix element $V_{fi} =< f|V|i >$, subject to energy conservation, and apart from normalization:

$$k = \frac{2\pi}{\hbar}\sum_{i;f}|V_{fi}|^2 e^{-E_i/k_BT}\delta(E_f - E_i) \qquad (3)$$

At room temperature $|i>$ will consist of a thermal mixture of Born–Oppenheimer states, the population of each being governed by a Boltzmann factor; each of these will interact with a bunch of Born–Oppenheimer states $|f>$ of the same energy within the resolution of the experiment. The delta function is thus to be interpreted as a density of states $\varrho(E_f)$. During the transfer the proton will move from the initial equilibrium position r_i along the tunneling mode r to the final equilibrium position r_f and from the initial vibrational level v of this mode to the final level w. Skeletal modes will play a role in this process. From results obtained for small molecules, we infer that their main effect is shortening of the transfer distance $r_f - r_i$ due to motion along vibrational coordinates or components thereof, collectively denoted by R, that are collinear with the tunneling mode r. For simplicity, we assume that the skeletal modes are basically the same in $|i>$ and $|f>$.

First we consider transfer of a proton or hydrogen atom along an adiabatic double-minimum potential involving a single electronic manifold. In terms of the Golden Rule, the coupling V can then be represented by an electronic term that may be taken independent of the vibrational coordinates. In that case the matrix element in Eqn (3) can be written in the form

$$V_{fi} = J < \Lambda(R)\chi_w(r - r_f)|\chi_v(r - r_i)\Lambda(R) > \qquad (4)$$

where, in our example, $< \chi_w(r - r_f)|\chi_v(r - r_i) >$ would be an R-dependent vibrational overlap integral between CH- and OH-stretch wavefunctions and $\Lambda(R)$ represents the set of skeletal vibrational wavefunctions with a component parallel to r. If the reaction is endothermic, the delta function in Eqn (3) generates a Boltzmann factor $\exp(-\Delta E^0/k_BT)$. If antisymmetric skeletal vibrations are coupled to the tunneling mode, they will contribute a similar Boltzmann factor. Such factors are isotope-independent and thus cancel if we consider the KIE.

In enzymatic reactions such as those of SLO1 where a redox system accepts an electron while the proton transfers, thereby putting the system into a new electronic state, the transfer is NA. To describe this transfer, we use a three-center model consisting of a substrate SH, where S represents the donor group, and the enzyme A–K consists of two connected parts, the proton-acceptor group A and the electron- withdrawing redox system K. The reaction can be symbolically depicted as

$$SH + A\text{-}K \rightarrow S^{\bullet} + HA^{+}\text{-}K^{-}$$

We assume that two electronic states, Φ_0 and Φ_1, are involved in the transfer and that their ordering changes from $E_i^{(0)} < E_i^{(1)}$ in the initial state $|i>$ to $E_f^{(1)} < E_f^{(0)}$ in the final state $|f>$, as illustrated in Fig. 7. Their energy separations are mostly governed by the properties of the redox system K. We assume further that their coupling is weak and is dominated at the crossing point along the proton-transfer coordinate r by the nuclear kinetic-energy term $\partial^2/\partial r^2$, leading to a dominant coupling matrix element

$$|V_{fi}^{NA}| =< \Phi_1|\partial/\partial r|\Phi_0 > \\ < \Lambda(R)\chi_w^{(1)}(r - r_f)|\partial/\partial r|\chi_v^{(0)}(r - r_i)\Lambda(R) > \qquad (5)$$

where we have used the same approximations as for adiabatic transfer. Since enzymatic reactions typically occur

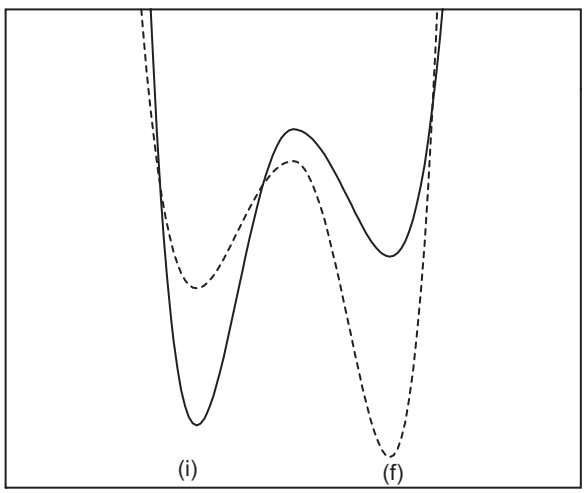

Figure 7. Schematic plot of two interacting double-minimum potentials used to describe nonadiabatic proton transfer in the systems under discussion

Table 1. Rate constants and activation energies at $T = 298$ K of soybean lipoxygenase-1 and six mutants calculated by linear regression from the kinetic data reported as Supporting Information in References [1, 2]

Enzyme	$\ln k^{H}$	$\ln k^{D}$	$\ln \eta$	E_a^H/k_BT	E_a^D/k_BT	$\Delta E_a/k_BT$
Linoleic/SLO1	5.7 ± 0.2	1.3 ± 0.3	4.4 ± 0.5	2.8 ± 0.5	5.3 ± 1.2	2.4 ± 1.7
Mutant I553A	5.7 ± 0.1	1.2 ± 0.4	4.5 ± 0.5	3.3 ± 0.7	8.6 ± 1.0	5.3 ± 1.7
Mutant I553L	5.8 ± 0.1	1.3 ± 0.3	4.5 ± 0.4	0.7 ± 1.2	6.7 ± 0.5	6.0 ± 1.7
Mutant I553V	4.3 ± 0.2	0.0 ± 0.4	4.3 ± 0.6	4.1 ± 0.9	8.3 ± 1.1	4.2 ± 2.0
Mutant I553G	4.1 ± 0.1	-1.2 ± 0.3	5.3 ± 0.4	0.0 ± 0.7	7.3 ± 0.7	7.3 ± 1.4
Mutant L546A	0.4 ± 0.2	-4.4 ± 0.4	4.8 ± 0.6	5.6 ± 0.4	9.3 ± 0.8	3.7 ± 1.2
Mutant L754A	-1.7 ± 0.3	-6.4 ± 0.4	4.6 ± 0.6	6.2 ± 0.8	8.9 ± 1.7	2.7 ± 2.5

at temperatures where CH- and CD-stretching vibrations are unlikely to be excited, we may set at least one of the quantum numbers (v, w) equal to zero. If $\chi_0^{(0)}(r - r_i)$ is taken to be a zero-point wavefunction, we obtain for a harmonic oscillator

$$|V_{fi}^{NA}| = J_{NA} < \Lambda(R)\chi_1^{(1)}(r - r_f)|r|\chi_0^{(0)}(r - r_i)\Lambda(R) > \qquad (6)$$

Here a_0 is the zero-point amplitude of the tunneling mode and the constants involved are absorbed into the constant J_{NA}, because we are concerned with relative rather than absolute values of the rate constants, specifically with their temperature and isotope dependence. The operator r raises the vibrational quantum number $\chi_0^{(0)}(r)$ by one unit, which may change (increase) the overlap substantially, but only through a pre-exponential factor.

Evolutionary arguments suggest that these reactions are unlikely to generate a net energy loss or gain as large as a quantum of these vibrations, which indicates that the other quantum number will be either zero or 1. It follows that the vibrational overlap integral S_{vw} of the tunneling mode will reduce to S_{00}, S_{01}, or S_{11}, all of which depend exponentially on the tunneling distance and differ only by pre-exponential factors. Since it will be our strategy to consider rate-constant *ratios*, including KIEs, rather than absolute rate constants, we go one step further and retain only the exponential part of the overlap integral, a procedure further justified in the Appendix. This allows us to treat adiabatic and NA reactions by the same model. Thus in the harmonic approximation we write the overlap integral of the tunneling mode in the form $\exp(-r^2/4a_0^2)$, where r is the transfer distance and $a_0 = \sqrt{\hbar/m\omega}$, m and ω being the mass and frequency of the CH or CD oscillator. Since we neglect its thermal excitation, we ascribe the temperature dependence of the rate constant for exothermic reactions exclusively to the contribution of skeletal modes to the transfer. The symmetric modes $\Lambda(R)$ modulate the instantaneous transfer distance $r = R - 2b$, R being the separation of the C and O atoms between which the hydrogen is exchanged and $2b$ being the sum of the CH and HO bond lengths. In addition, there may be antisymmetric modes that contribute a Boltzmann factor, which will also be essentially isotope-independent. For convenience we combine it with the Boltzmann factor for endothermic reactions $\exp(-\Delta E^0/k_BT)$ by replacing ΔE^0 by ΔE^{eff}. In this scheme the temperature dependence is the same for adiabatic and NA rate constants and is governed by ΔE^{eff} and the symmetric skeletal vibrations $\Lambda(R)$.

Since the modulation by these vibrations is slow compared to the hydrogenic vibration, we represent it by a distribution of R values. The simplest assumption we can make is that this distribution is normal, i.e., Gaussian:

$$P(R,T) = \frac{\exp\{-(R - R_0)^2/A^2(T)\}}{\sqrt{\pi}A(T)} \qquad (7)$$

Integration of the matrix element $|V_{fi}|$ over the distribution yields

$$< |V_{fi}|^2 > \simeq J^2 \exp\{-r_0^2/[2a_0^2 + A^2(T)]\} \qquad (8)$$

where $r_0 = R_0 - 2b$ is the equilibrium hydrogen transfer distance, i.e., the separation of the two hydrogen equilibrium positions, and J^2 includes the pre-exponential constants. In this approach the Arrhenius formula (2) is replaced by

$$\ln k(T) \simeq \ln\left[\frac{2\pi}{\hbar}J^2\varrho(E_f)\right] - \frac{r_0^2}{2a_0^2 + A^2(T)} - \Delta E^{eff}/k_BT \qquad (9)$$

which shows directly the relative contributions of the tunneling mode and the skeletal modes to the transfer path of length r_0. Thus the rate constant decreases exponentially with the square of the transfer distance scaled by the sum of the squares of the amplitudes of the modes contributing to the transfer. This result is general and does not depend on the details of the model.[7]

As a desirable refinement of the model, we formally introduce anharmonicity by replacing the zero-point amplitude of the tunneling mode $a_0^{H,D}$ by $a_{eff}^{H,D}$. For simplicity we set $m^D = 2m^H = 2$, so that $(a_{eff}^H)^2 = \sqrt{2}(a_{eff}^D)^2$.

To simplify the notation, we express all lengths in units a_{eff}^H and introduce new parameters

$$L = \ln\left[\frac{2\pi}{\hbar}J^2\varrho(E_f)\right]; \rho = \frac{r_0^2}{2(a_{eff}^H)^2}; z(T) = \frac{A^2(T)}{2(a_{eff}^H)^2}; \qquad (10)$$
$$B(T) = \Delta E^{eff}/k_BT$$

so that Eqn (7) reduces to

$$\ln k^H(T) = L - \frac{\rho}{1 + z(T)} - B(T),$$
$$\ln k^D(T) = L - \frac{\rho\sqrt{2}}{1 + z(T)\sqrt{2}} - B(T) \qquad (11)$$

In this notation $z(T)$ and $z(T)\sqrt{2}$ are the contributions of the skeletal modes to the transfer relative to the contribution of the H and D tunneling modes, respectively. Note that the form of Eqns (11) is not Arrhenius-like. Contrary to the Arrhenius

Eqn (2), they yield an expression for the KIE that has a clear physical meaning:

$$\ln \eta \equiv \ln k^{H}(T) - \ln k^{D}(T) = \frac{\rho(\sqrt{2}-1)}{[1+z(T)][1+z(T)\sqrt{2}]} \tag{12}$$

which means that the KIE increases exponentially with the square of the transfer distance and decreases exponentially with the skeletal modes contribution, the denominator of the exponent varying quadratically with $z(T)$ for $z(T) >> 1$ and roughly linearly with $z(T) < 1$.

We can use a corresponding approach to relate the rate constants for the same isotope in two different mutants:

$$\begin{aligned} \ln \frac{k_1^{H}(T)}{k_2^{H}(T)} &= -\frac{\rho_1}{1+z_1(T)} + \frac{\rho_2}{1+z_2(T)}, \\ \ln \frac{k_1^{D}(T)}{k_2^{D}(T)} &= -\frac{\rho_1\sqrt{2}}{1+z_1(T)\sqrt{2}} + \frac{\rho_2\sqrt{2}}{1+z_2(T)\sqrt{2}} \end{aligned} \tag{13}$$

provided we may assume that both the endothermicity term $B(T)$, if any, and the electronic term L are the same in the two mutants. For mutations close to the reaction center, this assumption clearly needs to be probed. However, since $k(T)$ is proportional to J^2, a change of the electronic factor by at least an order of magnitude would be required to account for the observed range of rate constants in terms of the electronic coupling. Such a large change following the replacement of one aliphatic side chain by another seems highly implausible. It follows that a change of L will be at most a minor correction. In that case substitution of Eqn (12) to eliminate the ρ parameter shows that if $\ln k_1^{H}(T) > \ln k_2^{H}(T)$ then $z_2(T)\ln\eta_2 > z_1(T)\ln\eta_1$. This implies that a mutation that reduces the activity of the enzyme will cause an increase in at least one of two parameters: $z(T)$, the contribution of the skeletal modes, and η, the KIE.

The equations derived thus far do not involve the temperature dependence of the observed properties and thus do not require a specific form for the parameter $A(T)$, which at the chosen temperature is just a number. However, to study the temperature dependence of the rate constants, we need to introduce such a form. Elsewhere[8] we have shown that in simple cases we can deal with the skeletal vibrations $\Lambda(R)$ that modulate the transfer distance $r_f - r_i$ in Eqns (4)–(6) by combining them into an *effective* mode, whose properties can be evaluated if a full force field calculation is available. Since this is usually not the case for enzymatic reactions, we follow the common procedure of fitting the effective frequency and reduced mass of this mode, which is often referred to as the gating or promoting mode, to the observed kinetic parameters. We assume that it is harmonic with an equilibrium position $R = R_0$, a frequency Ω and a reduced mass M. The model then allows us to derive values for these vibrational parameters from the observed temperature dependence of the transfer rate constants. In this approach the squared amplitude of the effective mode takes the form

$$A^2(T) = (\hbar/M\Omega)\coth(\hbar\Omega/2k_BT) \tag{14}$$

or, in dimensionless notation,

$$z(\xi) = \frac{(\hbar/M\Omega)}{2(a_{\text{eff}}^{H})^2}\coth\xi \tag{15}$$

where $\xi = \hbar\Omega/2k_BT$ measures the vibrational energy in terms of the thermal energy and thus represents a scaled inverse temperature. The distribution $z(\xi)$ replaces $z(T)$ when the contributing skeletal modes are represented by a single effective mode. Since this representation will tend to reduce skeletal-mode support, we expect that $z(\xi) \le z(T)$. In References [1, 2, 4, 5], a similar treatment is restricted to frequencies low compared to k_BT. Here we use a more general approach, which covers the full range of effective-mode frequencies. It will transpire that this is an essential generalization since it provides a test for the compatibility of a given data set with the adopted model.

Differentiating Eqns (11) with respect to the inverse temperature, and noting that $dT^{-1} = T^{-1}d\ln T^{-1}$, we obtain in dimensionless notation

$$-\frac{d\ln k^{H}(T)}{d\ln T^{-1}} \equiv \frac{E_a^{H}}{k_BT} = \rho\frac{z(\xi)F(\xi)}{[1+z(\xi)]^2} + B(T) \tag{16}$$

$$-\frac{d\ln k^{D}(T)}{d\ln T^{-1}} \equiv \frac{E_a^{D}}{k_BT} = \rho\frac{2z(\xi)F(\xi)}{[1+z(\xi)\sqrt{2}]^2} + B(T) \tag{17}$$

where $F(\xi) = \xi(\coth\xi - \tanh\xi)$ is a function that varies smoothly from 0 to 1, as illustrated in Fig. 8. This function, which depends only on the ratio $\hbar\Omega/k_BT$, represents the dependence of the model on the assumption that the effect of skeletal vibrations on the transfer dynamics can be approximated by that of a single effective harmonic oscillator with frequency Ω collinear with the tunneling mode. Any physical limits set on values of Ω imply corresponding limits on $F(\xi)$. Since $d\ln T^{-1} = TdT^{-1}$, the functions (16) and (17) can be read directly off conventional Arrhenius plots. *Note that these equations, in contrast to the Arrhenius equation, include the dependence of the observed activation energies on temperature.* Although this dependence may not be directly observable in the narrow temperature interval to which enzymatic systems are usually limited, it governs the ratio E_a^{D}/E_a^{H}:

$$\frac{E_a^{D} - \Delta E^{\text{eff}}}{E_a^{H} - \Delta E^{\text{eff}}} = 2\left[\frac{1+z(\xi)}{1+z(\xi)\sqrt{2}}\right]^2 \tag{18}$$

This expression depends only on the effective endothermicity, if any, and the relative contribution of the effective mode to the

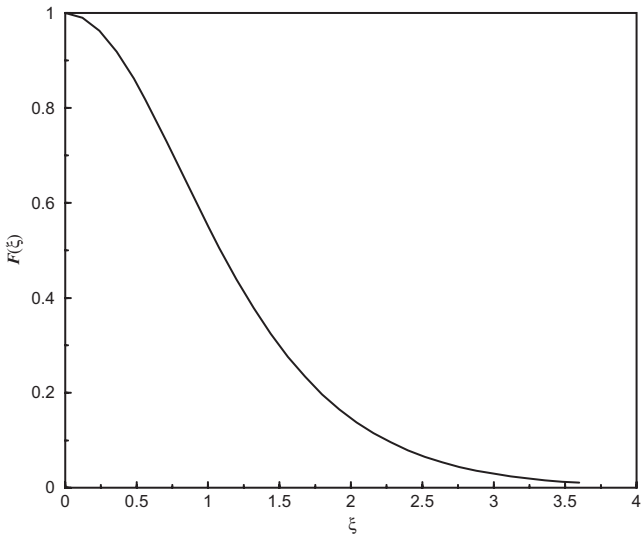

Figure 8. Plot of the effective-mode function $F(\xi) = \xi(\coth\xi - \tanh\xi)$, where $\xi = \hbar\Omega/2k_BT$

transfer. If the transfer is exothermic, as it is for SLO1 according to the argument presented in the preceding section, and if the contribution of antisymmetric modes is negligible, so that $B(T) \sim 0$, the ratio of Arrhenius slopes (18) will vary from 1 for large to 2 for small contributions. If $B(T) > 0$, the maximum value of this ratio will be less than 2. Since the activation energies measured in small temperature intervals tend to be subject to large experimental errors, the $z(\xi)$ values calculated from Eqn (18) may show large uncertainties.

The temperature dependence of the KIE is governed by the difference of Eqns (16) and (17),

$$\frac{d \ln \eta}{d \ln T^{-1}} \equiv \frac{\Delta E_a}{k_B T} = z(\xi) F(\xi) \rho \left\{ \frac{2}{[1 + z(\xi)\sqrt{2}]^2} - \frac{1}{[1 + z(\xi)]^2} \right\} \quad (19)$$

where $\Delta E_a = E_a^D - E_a^H$. This eliminates the dependence on any endothermicity, but maintains a dependence on the skeletal-mode function $F(\xi)$. In Fig. 9, $\Delta E_a / k_B T$ is plotted, along with $\ln \eta$, as a function of the contribution $z(\xi)$ for the parameter values $\rho = 25$ and $F(\xi) = 1$, whose numerical significance will be explored in the next section. Since both ΔE_a and $\ln \eta$ are linear functions of ρ, a change in the transfer distance does not affect the relation between the KIE and its temperature dependence and thus between the two curves in Fig. 9. By combining Eqns (12) and (19), one can readily show that $\Delta E_a / k_B T \leq 2 \ln \eta$, the limiting value being reached for large $z(\xi)$ and unit $F(\xi)$.

Although Fig. 9 is derived for specific values of the parameters $\rho(=25)$ and $F(\xi)(=1)$, it can be turned readily into a universal graph which can be used to test the compatibility of any enzymatic tunneling reaction with the two-oscillator model. Since, as pointed out above, a change of ρ does not change the relation between the two curves but only their numerical values, the graph remains valid for all ρ if we multiply the values along the abscissa by $\rho/25$. To accommodate values of $F(\xi)$ smaller than 1, we simply reinterpret the ΔE_a curve as $\Delta E_a / F(\xi) k_B T$. The values these parameters may assume are considered in the next section.

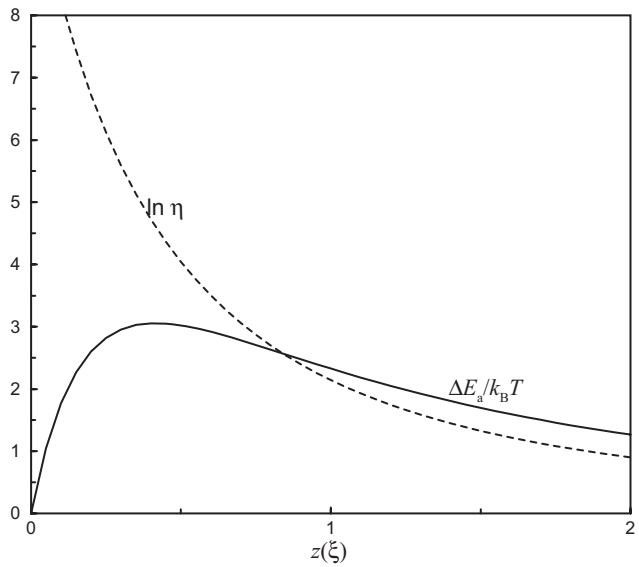

Figure 9. Plot of $\Delta E_a / k_B T$ (solid line) and $\ln \eta$ (broken line) against $z(\xi)$ for $\rho = 25$ and $F(\xi) = 1$. It becomes a universal graph for enzymatic tunneling reactions if the numbers along the abscissa are multiplied by $\rho/25$ and the solid line is reinterpreted as $\Delta E_a / F(\xi) k_B T$

Hence the treatment gives rise to three criteria for the compatibility of the data with the model:

(i) the effective-mode parameter $F(\xi)$ is limited to the range 0–1;
(ii) the temperature dependence of the KIE, given by $\Delta E_a / k_B T$, is limited to the range $0 - 2 \ln \eta$;
(iii) the effective activation energy at a given temperature for deuteron transfer cannot exceed twice that for proton transfer.

In addition there are numerical criteria relating the parameter ρ and thus the transfer distance to van der Waals radii and bond lengths, as discussed in the next section. Failure of a data set to meet these tests serves as a warning that it may not represent a single rate-determining tunneling step. Since the model parameters have a clear physical meaning, they can serve as a guide to trace the source of any discrepancy.

PARAMETER VALUES

Two key parameters of the model are the proton transfer distance r_0, i.e., the distance between the proton equilibrium positions in the initial and final state, and the zero-point amplitude of the proton in the two states, a_{eff}^H. In practice, the transfer distance can be reasonably estimated from standard bond lengths and van der Waals radii, and the zero-point amplitude from standard CH- and OH-stretching potentials. Together they determine the distance parameter ρ defined by Eqn (10). The van der Waals radius of the donating methylene group is about 2 Å and that of the accepting oxygen atom is about 1.4 Å. The standard CH-bond length is about 1.1 Å and the standard OH-bond length is about 1.0 Å. In the final state we expect that hydrogen bonding will reduce the C···O distance and increase the OH-bond length. In the initial state we expect little hydrogen bonding, but in the final state, which contributes on an equal footing in the Golden Rule approach, the ionic structure may lead to strong bonding. Therefore, we estimate the transfer distance (in Å) to be in the range $1.0 \leq r_0 \leq 1.2$. The zero-point amplitude a_0 for a harmonic oscillator with $m = 1$ and $\omega = 3000\ \text{cm}^{-1}$ equals 0.105 Å. Taking into account that the oscillator will be anharmonic and that the anharmonicity will increase with increasing hydrogen bonding, we estimate $0.11 \leq a_{eff} \leq 0.14$ Å. Combining these estimates, we arrive at $25 \leq \rho \leq 50$. These numbers are specific for the present system. Much larger values are expected, e.g., for proton transfer between two carbon centers.

For the effective mode that represents the contributing skeletal modes we envisage two limiting cases. In the presence of substantial hydrogen bonding, and thus small ρ values, it should closely resemble a localized C···H···O oscillator with an effective mass M that may approach the limiting value of about 7. The limiting frequency is difficult to estimate, since it is expected to be very different for the initial and final configuration, the latter being ionic. We note that a frequency of about $400\ \text{cm}^{-1}$, which seems very high for this type of van der Waals bond, would at 298 K translate into a value of about 0.55 for the function $F(\xi)$. Lacking more accurate information, we tentatively accept these estimates as our limit. Substituting these values together with the estimates of a_{eff}^H into Eqn (15), we obtain $z(\xi) \leq 1.0$ at 298 K. In systems with no significant hydrogen bonding, we expect large ρ values and small anharmonicity, together with contributions from a variety of low-frequency modes to the effective mode, resulting in a much larger effective mass, approaching that of the substrate,

and a frequency much smaller than the thermal energy of about 200 cm^{-1} at 298 K, which may give rise to $F(\xi)$ values close to the upper limit $F(\xi) = 1$. In this region the hyperbolic cotangent may be approximated by its inverse argument. We then obtain $z(\xi) \sim (m\omega/M\Omega)(k_BT/\hbar\Omega)$, which can assume a wide range of values at 298 K, depending on the properties of the effective mode. Thus in addition to the analytical compatibility criteria between model and data derived in the preceding section, numerical compatibility criteria can be derived from a proposed or generally accepted mechanism for a specific transfer reaction.

PROTOCOL

In this section, we consider the most efficient way to analyze a given data set in terms of the equations of the 'Model' section and the parameter estimates of the 'Parameter values' section. It will depend, of course, on the amount of information available. In the minimal case in which the data are limited to the KIE derived from product analysis and its activation energy, Fig. 9 indicates that additional information can be extracted only if $\Delta E_a/k_BT \geq \ln \eta$. This would imply a relatively large contribution $z(\xi)$ of the effective skeletal mode, which suggests that its frequency Ω is well below the thermal energy k_BT. In that case, $F(\xi)$ will be close to unity, so that it will be possible to estimate the transfer distance directly from Fig. 9, provided the data meet the compatibility criteria of the 'Model' section. From the transfer distance one may in turn be able to deduce the atoms between which the transfer is likely to occur and thus gain information on the transfer mechanism.

In cases where rate constants are available and enough is known about the mechanism to estimate the transfer distance by the approach of the 'Parameter values' section, the most efficient procedure is to start from this estimate and to use Eqn (12) to calculate $z(T)$, since the KIE value is likely to be more accurate than its activation energy. To interpret ΔE_a, one needs a model for the skeletal modes; our assumption that these modes can be represented by an effective mode is formally equivalent to the assumption that $z(T)$ can be replaced by $z(\xi)$. Then $F(\xi)$ can be obtained from ΔE_a and $z(\xi)$ by means of Fig. 9 or Eqn (19); similarly, the effective endothermicity can be obtained from Eqs (16)–(18). From $F(\xi)$ together with Eqn (15), one obtains the frequency Ω and the effective mass M of the effective mode. If all these results are mutually consistent, meet the compatibility criteria of the 'Model' section, and are numerically in line with physical expectations, the analysis is complete. Its conclusion will be that the tunneling step investigated is indeed rate limiting and that the numerical results will provide estimates for the tunneling distance, the effective endothermicity, and the properties of the effective mode supporting the tunneling.

If inconsistencies occur that lie outside the range of experimental uncertainties, it may be unclear how to proceed, especially if the data set is very small. As the measurements are very difficult and the model is undoubtedly oversimplified, there are many possible sources of error. In the next section, where we analyze the chosen system, several difficulties of this type are encountered. Their treatment, however tentative, is offered as an example of how they may be resolved. If the data set consists of several closely related reactions, it may be profitable not to deal with each reaction separately, but to deal first with the analysis of the rate constants at a single temperature, chosen near the middle of the range of temperatures for which measuments are available, since this information tends to be more accurate than that pertaining to the temperature dependence. This is the procedure we use in the following analysis of the SLO1 data.

ANALYSIS

We now probe whether the data set of Table 1 is compatible with the model of the 'Model' section for the range of parameter values estimated in the 'Parameter values' section. We start with a comparative analysis of the mean values of the rate constants at $T = 298$ K for the seven enzymes listed. If we may assume that evolution tends to optimize the efficiency of enzymes, it follows that the WT enzyme and the mutants I553A and I553L, which show the highest rates in Table 1, should be associated with the shortest proton transfer distance and thus the lowest values estimated for the parameter ρ. Tentatively setting $r_0 \simeq 1.00$ Å and $a_{\text{eff}} \simeq 0.14$ Å, so that $\rho = 25$, the lower limit deduced in the 'Parameter values' section, we can use Eqn (12) to calculate the contribution of the skeletal modes to the reaction path: $z(298) = 0.42 - 0.44$, i.e., roughly half as much as that of the tunneling mode. This result is compatible with the estimated range of the preceding section. Larger values of ρ, which yield larger values of $z(T)$, were tried, but for reasons that will become clear in the course of the analysis, they proved less satisfactory.

Since the three most active enzymes have virtually the same rate constants for proton as well as for deuteron transfer, and thus the same KIE, one is tempted to deduce that these mutations have no effect on the kinetics of the enzyme, a deduction supported by the observation that the mutations occur at a site not close to the reaction center. However, the substrate, linoleic acid, is a large molecule with a reach that may well extend to this remote region. This may explain why two mutants, I553V and I553G, with similar mutations at the same site, do exhibit a reduced activity, with rates smaller by factors of 4 and 5.5 for H and 3.5 and 12 for D, respectively. To probe whether these reductions, if real, should be ascribed to an increase in ρ or a decrease of $z(T)$, we use Eqn (15) together with Eqn (12) to relate the remaining enzymes to the top three. Since the mutations occur at a remote site, we assume that the electronic parameter L is not affected. Using the observed rate constants and KIEs listed in Table 1, we obtain for the mutant I553V: $z(298) = 0.60 \pm 0.08$ and $\rho = 31 \pm 2$, and for the mutant I553G: $z(298) = 0.38 \pm 0.07$ and $\rho = 26 \pm 2$; these numbers are collected in Table 2.

The result for I553V thus ascribes the reduced activity to a small increase in the transfer distance partly compensated by an increase in the contribution of the skeletal modes. Although it is not clear why this particular mutant should exhibit an increased transfer distance, the resulting increase in the skeletal modes contribution is in agreement with the notion that a weaker hydrogen bond would increase the frequency of the tunneling mode and decrease that of the effective skeletal mode, both of which would increase $z(T)$, as follows from Eqn (12). For the I553G mutant, the reduced activity is accompanied by an increase in the KIE that is large enough to imply a decrease in $z(T)$, such that the transfer distance remains essentially unchanged. There is no obvious rationale for the implied increase in the vibrational force constant other than a possible effect on the structure of the enzyme–substrate complex, since a weakening of the hydrogen bonding, suggested by the reduced activity, would have the opposite effect.

Table 2. Physical parameters of the model extracted from the data listed in Table 1

Enzyme	ρ	$z(298)$	$F(\xi)$	ξ	Ω/cm^{-1}	M/m^{H}
Lin./SLO1	(25)	0.44 ± 0.06	0.63 ± 0.10	0.87 ± 0.15	350 ± 80	14 ± 4
Mut. I553A	(25)	0.43 ± 0.06	~ 1	Small	Small	Large
Mut. I553L	(25)	0.42 ± 0.06	0.81 ± 0.07	0.56 ± 0.05	220 ± 30	32 ± 3
Mut. I553V	31 ± 2	0.60 ± 0.08	0.76 ± 0.10	0.65 ± 0.10	260 ± 50	17 ± 4
Mut. I553G	26 ± 2	0.38 ± 0.06	0.87 ± 0.10	0.45 ± 0.06	180 ± 40	52 ± 10
Mut. L546A	37 ± 3	0.65 ± 0.10	0.88 ± 0.10	0.44 ± 0.05	180 ± 50	31 ± 8
Mut. L754A	53 ± 4	1.0 ± 0.2	0.59 ± 0.15	0.93 ± 0.20	370 ± 80	6 ± 2

Values of ρ in brackets are chosen estimates.

Our result contradicts the large increase in the transfer distance r_0 for the mutants calculated in Reference [2]. As pointed out in the 'Parameter values' section, a transfer distance $r_0 = 0.66$ Å as proposed for the WT enzyme is incompatible with the known van der Waals radii and bond lengths of the groups directly involved in the transfer. Similarly, the value $r_0 = 2.55$ Å proposed for the I553G mutant is incompatible with the observed rate, which remains close to that of the WT. Equally surprising is the value $r_0 = 1.24$ Å assigned to the I553A mutant whose rate constants for H and D transfer are virtually the same as the corresponding WT rate constants. To reconcile the small rate changes with the large changes proposed for the transfer distance, the authors invoke 'conformational sampling', a concept originally introduced by Bruno and Bialek,[9] who modified a conventional one-dimensional tunneling model by replacing r_0 by empirical values that are different for H and D transfer in order to account for the contribution of skeletal vibrations to the rate; formally, this procedure is equivalent to the one we use in the 'Model' section. In terms of our model, these values amount to $r_0/\sqrt{1+z(T)}$ for H and $r_0/\sqrt{1+z(T)\sqrt{2}}$ for D transfer, as follows directly from Eqn (11). For the three enzymes quoted, whose $z(T)$ values are listed in Table 2, the corresponding values are $(0.85 \pm 0.01)r_0$ and $(0.80 \pm 0.01)r_0$, respectively, thus showing none of the large variations obtained in Reference [2]. Hence, the discrepancy can be traced back to the way the contribution of the skeletal modes is evaluated. While our evaluation is based on the KIE and estimates of the transfer distance based on standard van der Waals radii and bond lengths, that in Reference [2] apparently involves the activation energies; these we avoided here because of the large experimental uncertainties. Since the rate constants and KIEs in the I553 series show only modest variations, Occam's razor suggests that the same applies to the transfer distances, a suggestion to be tested in the remainder of the analysis.

The mutants L546A and L754A, whose mutations are at sites closer to the reaction center, show strongly reduced activity, namely by two and three orders of magnitude, respectively, for both H and D transfer. Such a large reduction following the replacement of a single nonpolar side chain cannot plausibly be ascribed solely to a change in electronic coupling and thus implies an increase in the transfer distance. The observation that this increase is not accompanied by a corresponding increase of the KIE indicates an increase in the contribution $z(T)$ of the skeletal vibrations, as follows from Eqns (12) and (13). If we ignore a possible change in electronic coupling, we can apply these equations to obtain $z(298) = 0.65 \pm 0.10$ and $\rho = 37 \pm 3$ for mutant L546A, and $z(298) = 1.0 \pm 0.2$ and $\rho = 53 \pm 5$ for mutant L754A, as listed in Table 2. We note that all these ρ values, except the last, remain within the estimate based on van der Waals radii and bond lengths $1.0 \leq r_0 \leq 1.2$ presented in the 'Parameter values' section, the corresponding increase in the transfer distance being in the range 0.10−0.15 Å. However, it seems likely that such changes would reduce the electronic coupling, especially in the case of the least active mutant, in which case the deduced values of $z(298)$ and ρ would be smaller.

Comparing all these results for $z(298)$ and ρ in Table 2, we note that their ratio turns out to be nearly constant. According to Eqn (8), this implies that the ratio $A(T)/r_0$ is nearly constant as well. In other words, among most of the mutants a change in the transfer distance is accompanied by a corresponding change in the force field of the effective skeletal mode, both being apparently associated with a change in hydrogen bonding. Since for the range of skeletal-mode contributions $z(T)$ encountered in these enzymes the denominator in Eqn (12) is an approximately linear function of $z(T)$, this implies that the KIE will be nearly constant for a wide range of rate constants.

The results collected in columns 2 and 3 of Table 2 do not depend directly on the temperature dependence of the rate constants; they are thus independent of the specific form chosen for the skeletal modes. To proceed, we need to use the observed activation energies and to apply the complete model in which the set of contributing skeletal vibrations is replaced by a single effective harmonic mode, so that $z(T)$ is restrained to $z(\xi) \leq z(T)$. If we set $z(\xi) = z(T)$ and use the values in Table 2 together with the ΔE_a values of Table 1, we can use Fig. 9 or Eqn (19) to calculate $F(\xi)$. This procedure works satisfactorily for the two inactive enzymes, where it leads to the $F(\xi)$ values listed in Table 2. However, it fails for the five active enzymes since it leads to values (much) larger than the limiting value of 1, implying that these data are incompatible with the model and thus with the assumption that the tunneling step is rate limiting. The assumption $z(\xi) < z(T)$ increases the discrepancy. Similarly, applying Eqn (18), we find that most of the active enzymes exceed the limiting value $E_a^{\mathrm{D}} \leq 2E_a^{\mathrm{H}}$.

To find the source of this discrepancy, we substitute $z(\xi) = z(T)$ in Eqns (16) and (17). As pointed out in the 'Summary of data' section, the small activation energies imply that the reaction is exothermic, so that we can set $B(T) = 0$; obviously,

setting $B(T) > 0$ would further complicate the problem. Using the rate constants listed in Table 1, we then calculate $F(\xi)$, which should be isotope-independent. We find, however, that for the active enzymes it is consistently smaller for H than for D transfer. Small $F(\xi)$ values imply large effective-mode frequencies; in the case of H transfer, they lead to frequencies well above our assumed limiting value of 400 cm^{-1}, while for D transfer they remain well under this limit. This suggests that the source of the discrepancy is to be found in the activation energies for H transfer, a suggestion that is strongly supported by the observation that two of these energies are essentially zero, a value incompatible with any tunneling model.

Whether these anomalously low activation energies are an experimental artifact or a fundamental aspect of the reaction mechanism we cannot determine on the basis of the available data. The fact that the anomalous activation energies all refer to rate constants $\ln k(298) > 4$, the largest values in Table 1 may suggest that the corresponding values of k_{cat}^{H} are contaminated with the rate constant of one or more other steps in the reaction sequence, since, as argued in the 'Introduction' section, rates of rate-limiting steps in enzymatic reactions are under upward evolutionary pressure. If this is the case, the problem of the vanishing activation energies can be reduced to a problem in the kinetics rather than in the modeling. Be this as it may, it seems prudent at this stage, to continue the analysis without the E_a^H values of the WT enzyme and the I553 mutants. Their $F(\xi)$ values in Table 2 are therefore derived solely from Eqn (17) for deuteron transfer, while those for the two inactive mutants are derived from Eqn (18). All are now between the allowed limits 0 and 1, which indicates that the model is compatible with these data. From $F(\xi)$ we obtain ξ and thus the effective-mode frequency Ω; these parameters are listed in columns 5 and 6 of Table 2. To obtain the mass M of the effective mode in atomic mass units, we set $z(\xi) = z(T)$ and substitute it together with ξ in Eqn (15). The results are listed in column 7.

These results show that both the frequency and the effective mass of the effective mode exhibit very large variations between the closely related enzymes. This is hardly realistic. Given the uncertainties of the observed activation energies and the rapid variation of ξ with $F(\xi)$ for $F(\xi) \geq 0.9$, the best we can do is ignoring the variations and taking averages. Excluding the least active enzyme for which there is evidence of a change in the electronic term L, this yields $\Omega_{av} \sim 200\ cm^{-1}$ and $M_{av} \sim 40$. These are reasonable numbers for the system, but they depend strongly on ρ. If we had started with $\rho = 30$ instead of 25, we would have obtained $\Omega_{av} > 300\ cm^{-1}$, which seems too high. If on the other hand, we had adopted a value of ρ smaller than 25, several additional mutants would have exhibited $F(\xi)$ values above the limiting value of 1, leading to a drastically reduced average frequency. These results further justify the present choice of ρ values.

CONCLUSIONS

This contribution aims to show that tunneling, which is ubiquitous in enzymatic proton-transfer reactions, provides a hitherto underused tool to investigate the mechanism of these reactions. The availability of two rate constants for basically the same reaction, differing only through the mass of the proton, can be exploited by suitable modeling. The model we use has been around for decades, but the possibility to cast it in an analytical form that allows direct comparison with kinetic data has not been explored before. In the form used here it offers criteria for deciding whether a given data set can be assigned to a single step in a reaction sequence. If so, it can derive information of the transfer mechanism such as the transfer distance and the part played by skeletal vibrations in the transfer. It can also explore changes in the mechanism due to mutations in the enzyme or variation of the substrate.

To demonstrate how the model works in practice, we analyzed the kinetic SLO1 data reported by Klinman and coworkers[1,2] In this reaction proton transfer is driven by the abstraction of an electron from the CH bond by an iron-based redox system. The reaction is NA and its rate depends on terms not included in the model. However, in an Appendix we show that these terms roughly cancel if we consider only relative rate constants. As shown in Table 2, the analysis of the data set requires only a single adjustable parameter, which, moreover, is not chosen freely but derived from physical parameters that can be reliably estimated. Even this parameter can be eliminated if the data are sufficiently accurate.

The kinetic data reported in References [1, 2] form a set that is unique because of the many mutants that were investigated. They show a number of intriguing features, including vanishing activation energies for some mutants and large variations in transfer rates not accompanied by corresponding changes in the KIE. The analysis suggests that the smallest activation energies, which are associated with the highest rates of ^1H transfer, may refer to tunneling steps contaminated by other steps in the reaction sequence. The transfer distance between the two proton equilibrium positions is estimated to be about 1.0 Å for the WT enzyme and up to 1.15 Å for the least active mutant. The properties of the skeletal modes assisting the tunneling indicate that hydrogen bonding plays a major part in the transfer despite the expected very weak hydrogen bonding in the initial configuration. This follows both from the values derived for the effective-mode frequencies and from the similarity of the KIE for active and inactive mutants. It is in line with the observation that proton transfer is accompanied by electron abstraction from the CH bond by the redox system. The remarkable constancy of the KIE among the mutants is traced back to the proportionality of the transfer distance and the force field of the C···H···O bond, as expected for a hydrogen-bonded system.

The analysis shows that specific answers can be obtained if a sufficiently rich set of kinetic data is interrogated by the model of the 'Model' section. The equations required for the analysis are elementary and can be applied directly to the observed rate constants and their temperature dependence. However, the accuracy of individual rate constants and, especially, activation energies tends to be limited owing to the complexity of the enzymatic processes. Data sets pertaining to several closely related reactions are therefore of particular interest but, unfortunately, few of these are presently available.

APPENDIX

In this Appendix, we consider the pre-exponential terms in the expression for the transfer rate constant, which were neglected in the 'Model' section. First we consider adiabatic transfer for

which the coupling V driving the transfer is an electronic term that may be taken independent of the vibrational coordinates. In that case the vibrational integral reduces to an overlap integral. Integrating the zero-point level overlap integral s_{00} over the distribution (7) to obtain the squared matrix element (8), we neglected a pre-exponential factor of the form $\sqrt{2a_0^2/[2a_0^2+A^2(T)]}$. Including this term leads to corrections to Eqn (11):

$$\ln k^{\mathrm{H}}(T) = L - \frac{\rho}{1+z(\xi)} - \frac{1}{2}\ln[1+z(\xi)] - B(T) \qquad \text{(A1)}$$

$$\ln k^{\mathrm{D}}(T) = L - \frac{\rho\sqrt{2}}{1+z(\xi)\sqrt{2}} - \frac{1}{2}\ln[1+z(\xi)\sqrt{2}] - B(T) \qquad \text{(A2)}$$

and thus also to Eqn (12):

$$\ln \eta = \frac{\rho(\sqrt{2}-1)}{[1+z(\xi)][1+z(\xi)\sqrt{2}]} - \ln C \qquad \text{(A3)}$$

where

$$C = \left[\frac{1+z(\xi)}{1+z(\xi)\sqrt{2}}\right]^{1/2} \qquad \text{(A4)}$$

In general these are small corrections that do not influence the results significantly. The temperature dependence of these corrections is negligible for our purpose.

For NA transfers, the corrections tend to be larger than for adiabatic transfers, since the overlap integral of the tunneling mode is of the form s_{01}. Carrying out the integration over the distribution (7) we obtain instead of Eqn (8)

$$\left\langle |V_{fi}|^2 \right\rangle = J_{\mathrm{NA}}^2 \frac{a_0 r_0^2}{[2a_0^2+A^2(T)]^{3/2}} \exp\left(-\frac{r_0^2}{2a_0^2+A^2(T)}\right) \qquad \text{(A6)}$$

which modifies Eqns (11) and (12) to

$$\ln k^{\mathrm{H}}(T) = L - \frac{\rho}{1+z(\xi)} + \ln\frac{\rho}{2[1+z(\xi)]^{3/2}} - B(T)$$

$$\ln k^{\mathrm{D}}(T) = L - \frac{\rho\sqrt{2}}{1+z(\xi)\sqrt{2}} + \ln\frac{\rho\sqrt{2}}{2[1+z(\xi)\sqrt{2}]^{3/2}} - B(T) \qquad \text{(A7)}$$

and

$$\ln \eta = \frac{\rho(\sqrt{2}-1)}{[1+z(\xi)][1+z(\xi)\sqrt{2}]} - 3\ln C - \ln\sqrt{2} \qquad \text{(A8)}$$

It follows that for the $z(T)$ values in Table 2 the correction terms to the KIE nearly cancel; however, corrections to absolute values of the rate constants may be substantial. The temperature dependence of the correction terms in Eqn (A8) follows from

$$\frac{d\ln[1+z(\xi)]}{d\ln T^{-1}} = \frac{z(\xi)}{1+z(\xi)}F(\xi) \qquad \text{(A9)}$$

and the equivalent equation with $z(\xi)$ replaced by $z(\xi)\sqrt{2}$; these terms are always smaller than unity. Introducing the NA corrections in Eqns (16) and (17) we obtain

$$\frac{E_a^{\mathrm{H}}}{k_B T} = \frac{z(\xi)F(\xi)}{[1+z(\xi)]^2}\left\{\rho - \frac{3}{2}[1+z(\xi)]\right\} + B(T) \qquad \text{(A10)}$$

$$\frac{E_a^{\mathrm{D}}}{k_B T} = \frac{2z(\xi)F(\xi)}{[1+z(\xi)\sqrt{2}]^2}\left\{\rho - \frac{3}{2}[1+z(\xi)\sqrt{2}]\right\} + B(T) \qquad \text{(A11)}$$

leading to

$$\frac{E_a^{\mathrm{D}} - \Delta E^0}{E_a^{\mathrm{H}} - \Delta E^0} = 2C^4 \frac{\rho - \frac{3}{2}[1+z(\xi)\sqrt{2}]}{\rho - \frac{3}{2}[1+z(\xi)]} \qquad \text{(A10)}$$

instead of Eqn (18) and

$$\frac{\Delta E_a}{k_B T} = z(\xi)F(\xi) \times \left\{\frac{2\rho}{[1+z(\xi)\sqrt{2}]^2} - \frac{\rho}{[1+z(\xi)]^2} - \frac{3}{2}\frac{1+z(\xi)(2-\sqrt{2})}{[1+z(\xi)][1+z(\xi)\sqrt{2}]}\right\} \qquad \text{(A12)}$$

instead of Eqn (19). It follows that for the parameter values in Table 2 the new terms may reduce the activation energies and their difference by up to 10%, which is generally within the margin of experimental error; however, they do not significantly affect their ratio.

As a result the numerical estimates of the 'Analysis' section remain valid within the accuracy of the data and the model. Whereas the NA corrections may increase the absolute values of the rate constants by an order of magnitude, and decrease their effective activation energies by 10%, they have only a minor effect on isotope effects and their temperature dependence as well as the relative efficiency of closely related enzymes.

REFERENCES

[1] M. J. Knapp, K. W. Rickert, J. P. Klinman, *J. Am. Chem. Soc.* **2002**, *124*, 3865.
[2] M. P. Meyer, D. R. Tomchick, J. P. Klinman, *Proc. Natl Acad. Sci. U. S. A.* **2008**, *105*, 1146.
[3] W. Siebrand, T. A. Wildman, M. Z. Zgierski, *J. Am. Chem. Soc.* **1984**, *106*, 4083, 4089.
[4] W. Siebrand, Z. Smedarchina, *J. Phys. Chem. B* **2004**, *108*, 4185.
[5] W. Siebrand, Z. Smedarchina, in *Isotope Effects in Chemistry and Biology* (Eds: A. Kohen, H.-H. Limbach), CRC Press, Boca Raton, **2006**, p. 725.
[6] A. M. Kuznetsov, J. Ulstrup, *Can. J. Chem.* **1999**, *77*, 1085.
[7] Z. Smedarchina, W. Siebrand, *Chem. Phys. Lett.* **2005**, *410*, 370.
[8] Z. Smedarchina, W. Siebrand, *Chem. Phys.* **1993**, *170*, 347.
[9] W. J. Bruno, W. Bialek, *Biophys. J.* **1992**, *63*, 689.